Infrared Physics & Technology 126 (2022) 104353

Contents lists available at ScienceDirect

Infrared Physics and Technology

journal homepage: www.elsevier.com/locate/infrared

Unmanned airborne miniaturized pulsed CO_2 laser with wavelength automatic tuning

Qikun Pan [a], Yang Gao [a,b], Deyang Yu [a], Kuo Zhang [a], Ranran Zhang [a], Chongxiao Zhao [a], Jin Guo [a], Fei Chen [a,*], Chunlei Shao [a,*]

[a] State Key Laboratory of Laser Interaction with Matter, Changchun Institute of Optics, Fine Mechanics and Physics, Chinese Academy of Sciences, Changchun 130033, China

[b] University of Chinese Academy of Sciences, Beijing 100049, China

ARTICLE INFO

Keywords:
CO_2 laser
Mechanical Q-switching
Wavelength tuning
Miniaturization integration

ABSTRACT

This paper presents a miniaturized mechanically Q-switched pulsed CO_2 laser with wavelength automatic tuning, which could be used in unmanned airborne lidar system. A three-mirror cavity structure with real focus in the cavity is designed to provide a stable resonator, which has short beam transit time for mechanically Q-switched laser. The matching relationship between the beam in the resonant cavity and the aperture of the optical chopper is experimentally studied, the CO_2 laser pulse output with good waveform is obtained, and the wavelength automatic tuning is realized. The CO_2 laser produces a maximum output peak power of 3.7 kW at 10.59 μm for pulse width of 350 ns, corresponding beam quality M^2 of 1.75, and the laser weight is about 18 kg.

1. Introduction

CO_2 laser has the advantages of high output power, good spectral purity and easy pulse modulation. It plays an important role in the fields of ultra-precision optical material processing, laser etching, EUV lithography and strong-field physics regime [1–5]. And the tunable CO_2 laser has gained widespread attention in the differential absorption lidar (DIAL), which primarily due to its rich spectral lines covering absorption peaks of various gases [6–10].

A DIAL probes the atmosphere with pulsed laser radiation at two closely spaced wavelengths, one coinciding with an absorption line of the trace gas and the other in the wing of this absorption line. The difference in intensity of the return signals can be used to deduce the concentration of the constituent of interest. In order to avoid the influence of atmospheric jitter, the laser needs to be tuned quickly. A rapidly tunable pulsed CO_2 laser based on two oppositely placed acoustic-optic modulator was reported in [6], where two wavelengths emitted from different oscillation paths with time interval of 1 ms. A mobile lidar system consisting of two pulsed TEA CO_2 lasers for detecting chemical warfare agents was reported in [7], which system volume was 7 m × 2.5 m × 3 m, and the detection distance was about 1 km. In [8], a CW tunable CO_2 laser DIAL system has been developed, and the back-scattered returns were measured from a retroreflector array target with distance of 0.1 km. In [9], a helicopter-borne lidar based on pulse-periodic mini-TEA CO_2 laser was demonstrated, that volume was 500 mm × 600 mm × 700 mm, and the detection distance was about 1 km with electric power consumption of 1 kW.

When DIAL system is used for detecting chemical warfare agents, a little carelessness will cause fatal injury to the operator [10]. The unmanned airborne DIAL system avoids the direct contact between personnel and the environment, which is one of the best methods for remote detection of toxic gases [11,12]. At present, due to lack of miniaturized high peak power tunable pulsed CO_2 laser with low power consumption, there is no report of CO_2 laser DIAL system applicable to unmanned airborne environment.

In this paper, a miniaturized pulsed CO_2 laser with wavelength automatic tuning was demonstrated. By inserting an optical chopper into the three-mirror cavity, the mechanically Q-switched CO_2 laser was presented with maximum peak power of 6.6 kW under non wavelength tuning regime. Under grating tuning regime, 37 lines was obtained at the range of 9.2 μm −10.71 μm, with corresponding peak power of 3.7 kW at 10.59 μm. The laser weight was about 18 kg with maximum electric power consumption of 145 W.

* Corresponding authors.
E-mail addresses: feichenny@126.com (F. Chen), sclem@sina.com (C. Shao).

https://doi.org/10.1016/j.infrared.2022.104353
Received 11 July 2022; Received in revised form 8 September 2022; Accepted 10 September 2022
Available online 16 September 2022

2. Resonator design for mechanical Q-switching

Intracavity Q-value modulation is an effective way to realize CO_2 laser pulse output. Both acousto-optic [13] and electro-optic [14] Q-switched CO_2 laser have good pulse modulation effect. The acousto-optic modulator has higher electric power consumption, and the electro-optic modulator need higher driving voltage. These shortcomings limit their application in complex environments. Mechanically Q-switched CO_2 laser using optical chopper, which has low electric power consumption and no heat dissipation, is required. So, mechanical Q-switching looks very attractive for miniaturized pulsed CO_2 lasers.

Due to the slow mechanical rotation speed of the optical chopper, the optical resonator needs to be specially designed to match the beam in the cavity and the optical aperture of the chopper. Malov reported a 4-mirror folded cavity to transform the beam in the cavity to match the optical chopper, and realized high repetition rate pulsed CO_2 laser output [15]. The 4-mirror folded cavity is relatively complex, which brings great difficulties to laser installation and miniaturization. In this paper, a three-mirror linear cavity structure with real focus in the cavity is proposed, which is composed of rear mirror, focusing lens and output coupler. The optical layout is shown in Fig. 1. The curvature radius of the spherical rear mirror is R, and the focal length of the focusing lens is f. The spherical center of the rear mirror coincides with the focal length of the focusing lens ($L_1 = R + f$). The real focus in the cavity is properly used by the optical chopper to effectively compress the response time of mechanical Q-switching. The output coupler could be a plane ZnSe lens or a plane grating, which distance from the focusing lens is L_2.

The stability of three mirror cavity is analyzed by ABCD matrix method. The transfer matrix of light in the resonant cavity is given by the product of the unit transfer matrix.

$$M = \begin{bmatrix} A & B \\ C & D \end{bmatrix} = \begin{bmatrix} 1 & 0 \\ 0 & -1 \end{bmatrix} \begin{bmatrix} 1 & -L_2 \\ 0 & 1 \end{bmatrix} \begin{bmatrix} 1 & 0 \\ 1/f & 1 \end{bmatrix} \begin{bmatrix} 1 & -L_1 \\ 0 & 1 \end{bmatrix} \begin{bmatrix} 1 & 0 \\ 2/R & -1 \end{bmatrix} \begin{bmatrix} 1 & L_1 \\ 0 & 1 \end{bmatrix} \begin{bmatrix} 1 & 0 \\ -1/f & 1 \end{bmatrix} \begin{bmatrix} 1 & L_2 \\ 0 & 1 \end{bmatrix} \tag{1}$$

The transfer matrix of light after n round trips in the resonant cavity is Mn. According to laser principle and matrix theory, the stability condition of laser resonator can be written as [16]:

$$(0.5A + 0.5D)^2 \leqslant 1 \tag{2}$$

Numerical simulation of the resonator stability condition was implemented. The length L_2 is determined by the length of gain region. In this paper, the real length of the gain region is 900 mm. The calculation results of cavity stability under different combination parameters of rear mirror and focusing lens are shown in Fig. 2. Rx-Fy represents that the curvature radius of the rear mirror is x mm and the focal length of the focus lens is y mm. Considering miniaturization, we keep the total cavity length unchanged. Under different combination conditions, the resonator is stable when $x + y = L_1$. However, with the increase of R and shortening of f, the variable range of the resonator length corresponding to the stable region decreases gradually, and the anti-interference of the resonator gradually deteriorates. Considering that an optical chopper should be inserted, R cannot decrease indefinitely. In this design, we used the values of R24-F43, whose variable range of cavity length in the stable region increases by 63% compared with R33-F34. The insensitivity of the resonator to the length enriches the choice of laser shell materials. For example, aluminum alloy with low-density could be used to replace indium steel with low linear expansion coefficient, which provides a theoretical basis for the lightweight design of the laser.

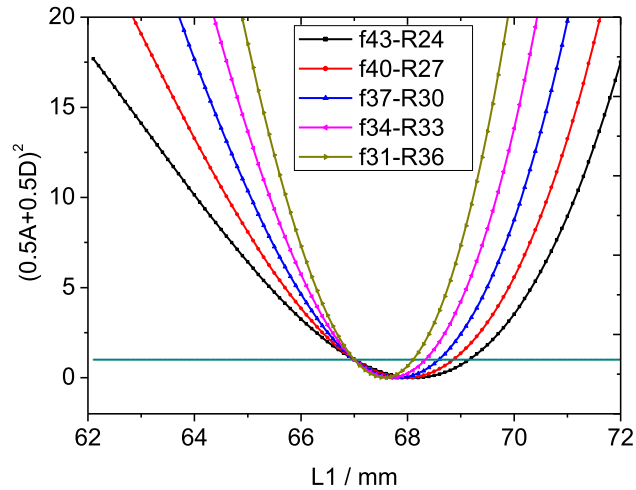

Fig. 2. Stability under different resonator parameters.

3. Experimental setup

The volume, weight and power consumption are fully considered in the design of the tunable pulsed CO_2 laser. The experimental setup is shown in Fig. 3, which is composed of three modules: wavelength tuning, laser gain and pulse modulation. The wavelength tuning module included a blazing grating and an electric turntable. The grating was a metal plane grating which has good thermal stability and high damage threshold. The scribed line of the grating was 100 L / mm, and the blaze angle was 28.71°, corresponding blaze wavelength was 9.6 μm. The grating adopted a working mode of first-order oscillation and zero order output, with first-order diffraction efficiency of about 80%. The grating and reflector 1 formed an angle reflector with an included angle of 60°. The angle reflector was mounted on a miniaturized and high-precision electric turntable. According to angle reflector principle, the transmission direction of CO_2 laser remains unchanged during wavelength tuning, which is convenient for lidar application. The Minimum incremental motion of the electric turntable was 0.001°, the Bi-directional (clockwise and counterclockwise directional) repeatability was ±0.005°, and the maximum speed was 20°/s.

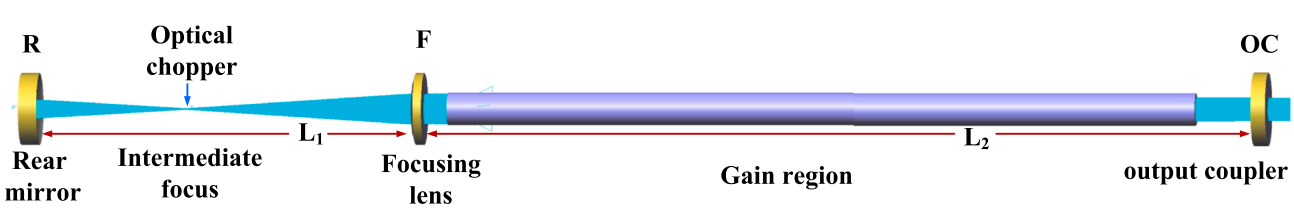

Fig. 1. A three-mirror linear cavity structure for mechanical Q-switching.

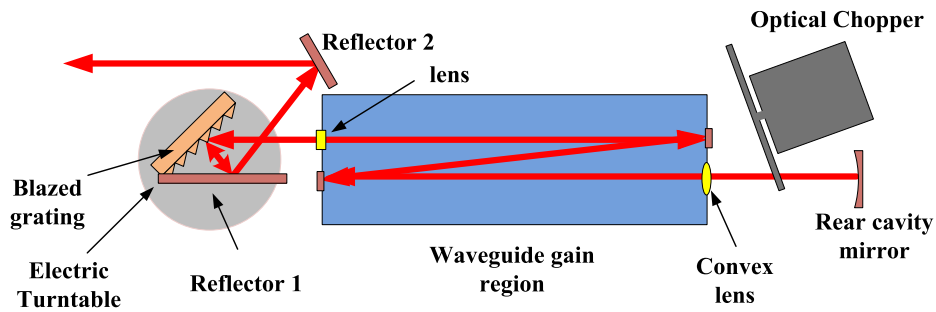

Fig. 3. Schematic experimental diagram of the tunable pulsed CO_2 laser.

The laser gain module adopted RF excitation mode with Z-shaped ceramic folding structure, which provides convenience for miniaturization design. The working voltage of the RF laser was 48 V DC, the modulation frequency was controlled by external trigger signal, and the adjustment range of RF excitation duty cycle was 1%−99%. The folding laser gain region adopted a plane mirror to turn the optical path, which does not affect the stability of the laser resonator.

The pulse modulation module was composed of a focusing lens, an optical chopper and a rear mirror. The focus of the focusing mirror coincides with the spherical center of the rear mirror. The chopper was located on the focal plane of the focusing lens, which can effectively compress the transit time of the chopper on the beam and improve pulse modulation characteristics of mechanically Q-switched laser. The maximum speed of the optical chopper motor was 6000 rpm. We have used chopper with 10 slits, which allowed us to obtain a maximum pulse repetition frequency up to 1 kHz. The optical chopper used a phased-locked loop (PLL) motor speed control design to accurately maintain the chopping speed as well as the phase of a reference signal, and stable frequency for reliable, long-term performance. Through the external synchronization signal, the chopper frequency can be matched with the excitation frequency of RF gain. The stable optical resonator system was composed of rear mirror, focusing lens and grating, which should improve the power stability of mechanically Q-switched CO_2 laser in unmanned airborne environment.

4. Experimental results

Firstly, we investigated the mechanical Q-switching characteristics of a RF excited CO_2 laser without wavelength tuning modular. A ZnSe flat lens with reflectivity of 20% was used as the output coupler. The slit width of the chopper has a significant impact on the modulation response time. In this study, we have used slit width with 0.4 mm, 0.8 mm 1.2 mm, which allowed us to obtain beams transit time of 13.8 μs, 27.6, 41.4 μs respectively. The effective diameter of the chopper was 92 mm, and the linear velocity was 28.9 m/s at rotation speed of 6000 rpm accordingly. A signal generator was used as the time synchronization control device to realize the working frequency matching of RF laser and optical chopper. The variation of average output power of mechanically Q-switched CO_2 laser with RF excitation duty ratio at 1 kHz was shown in Fig. 4.

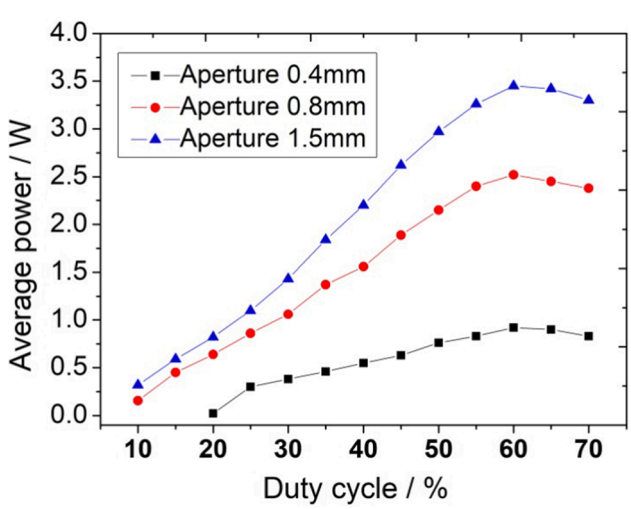

Fig. 4. The average output power of mechanically Q-switched CO_2 laser at 1 kHz.

As shown in Fig. 4, the average laser power of the mechanically Q-switched CO_2 laser increases linearly at lower duty ratio. However, when the duty ratio is greater than 60%, the average power begins to decrease slightly with the increase of the duty ratio. The upper-level lifetime of RF excited CO_2 laser is shorter than 1 ms, so more upper-level particles cannot be accumulated at higher duty ratio at 1 kHz. Meanwhile, with the increase of duty ratio, the thermal effect of air-cooled RF laser gradually appears, and the thermal relaxation process would lead to decrease of the average power. At the same RF duty ratio, the average power increases significantly with the increase of the slit width. The most obvious reason is that the insertion loss decreases gradually with the increase of slit width. In addition, the slit width of the chopper had a significantly effect on the laser pulse waveform. HgCdTe photodetector was used to test the laser pulse waveform under different slit widths, with results shown in Fig. 5.

Due to the same rotation speed of the chopper, the mechanically Q-switched pulse has a similar steep front waveform at different slit widths. The FWHM of laser pulse are about 330 ns, 350 ns and 390 ns at slit width of 0.4 mm, 0.8 mm and 1.2 mm, respectively. As the slit width increases, the tail of the laser pulse becomes more and more serious, and a secondary peak occurs at slit width of 1.2 mm. The long tail attached to pulse is a typical characteristic of slow response of CO_2 laser Q-switching device, which would decrease the laser peak power. Considering the average output power and pulse waveform of mechanically Q-switched CO_2 laser, silt width of 0.8 mm matches well with the focused beam in the cavity, and the maximum pulse peak power of 6.6 kW was obtained at 1 kHz. Fig. 5(D) shows the instability of pulse amplitude at maximum average power. The mechanical vibration of the optical chopper during high-speed rotation and the thermal relaxation process of RF excited laser gain are the main factors causing pulse energy amplitude jitter.

We investigated the automatic wavelength tuning characteristics of this mechanically Q switched CO_2 laser at slit width of 0.8 mm. According to grating equation, $2d\sin\theta = m\lambda$, incident angle θ of any spectral lines and the angular interval between lines could be calculated. For example, incident angles of 10.59 μm and 10.61 μm lines are 31.976° and 32.045° respectively, and the angle difference between them is about 0.069°. Through theoretical calculation of the incident angle of each spectral line and experimental correction, the corresponding relationship between the laser line and the rotation angle of the electric turntable could be established. So, the automatic tuning of CO_2 laser lines could be realized by software control.

The output spectrum of the mechanically Q-switched pulsed CO_2

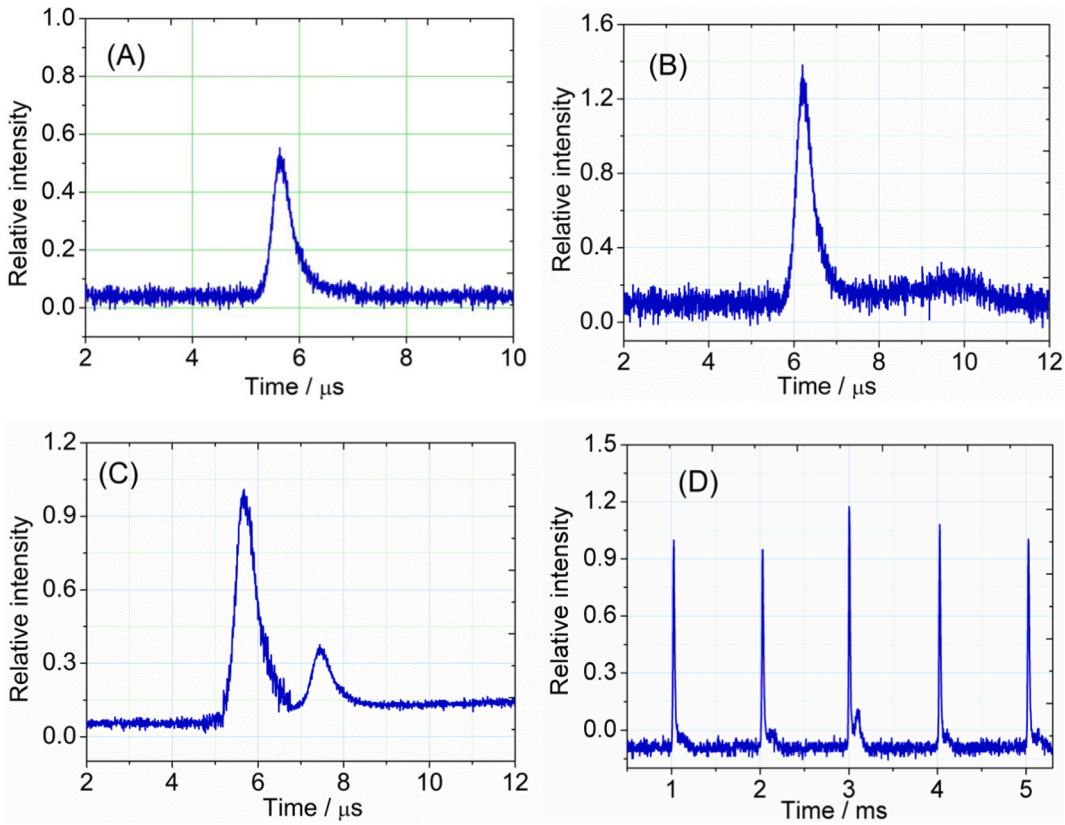

Fig. 5. Pulse waveform of mechanically Q-switched pulsed CO2 laser at different slit widths (A) 0.4 mm, (B) 0.8 mm, (C) 1.2 mm, (D) pulse train at 1 kHz with slit width of 0.8 mm.

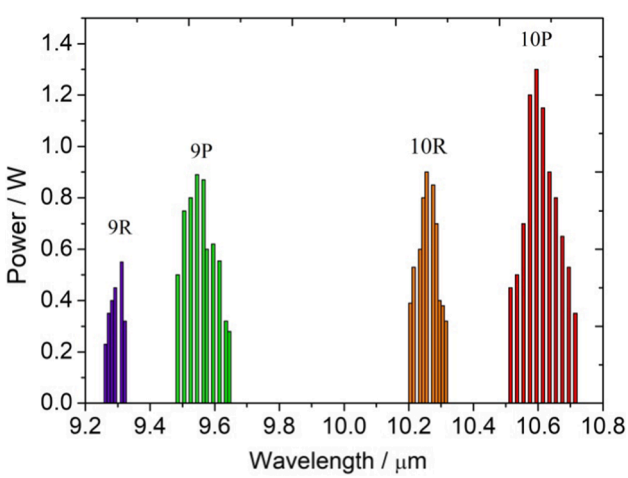

Fig. 6. Output spectrum of mechanically Q-switched pulsed CO_2 laser.

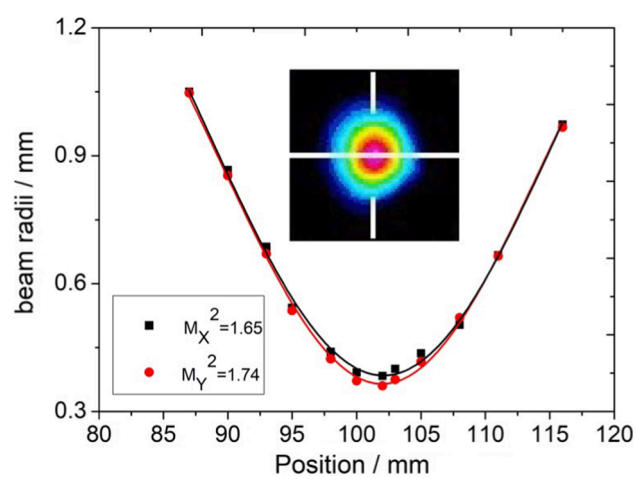

Fig. 7. The measurement of M^2 factor of CO_2 laser.

laser was tested by CO_2 laser spectrum analyzer, and the results are shown in Fig. 6. In range of 9.2–10.71 μm, 37 lines were measured, and the maximum average power was 1.3 W at 10.59 μm. The corresponding peak power was about 3.7 kW with pulse width of 350 ns. The automatic tuning time of adjacent spectral lines was about 50 ms. It is noteworthy that the average laser power decreases approximately linearly from 10p branch to 9R branch. Two reasons may account for this. Firstly, CO_2 laser has relatively strong laser gain in 10p branch. Secondly, the laser was integrated at the strongest line of 10.59 μm, and misalignment of the resonator would be caused by rotation of the turntable, and would gradually accumulate with the increase of rotation angle. By introducing a closed-loop correction device to compensate the resonator misalignment during the rotating motion, it is expected to obtain more

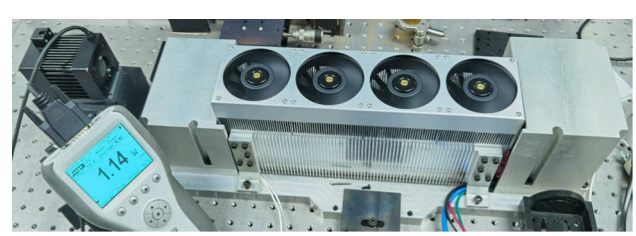

Fig. 8. The photo of miniaturized pulsed CO_2 laser with wavelength automatic tuning.

CO_2 laser spectral lines and improve laser power of the weak gain spectral lines.

The M^2 factor of this CO_2 laser at maximum output power was estimated by a DataRay camera. A lens with focal length of 100 mm was served to transform the output beam. The beam radius was recorded at different positions along the beam propagation direction, as shown in Fig. 7. The parametric of output beam was achieved by fitting the measured data. As a result, the beam quality factor at the maximum output power was hyperbolically fitted to be Mx^2~1.65 and My^2~1.74 along the horizontal and vertical directions respectively.

The miniaturized pulsed CO_2 laser with wavelength automatic tuning was integrated in our lab, just as shown in Fig. 8. The bottom plate was made of hollow aluminum alloy with thickness of 15 mm, which is beneficial to improve the stability of the laser under unmanned airborne environment. The integrated aluminum alloy support structure was adopted, which provides stable and reliable support for optical elements. Overall dimension of the laser is 520 mm × 192 mm × 160 mm, the weight is 18 kg, and the power consumption is 145 W. Outdoor experiments showed that the laser can work properly in the unmanned airborne environment.

5. Conclusions

In conclusion, this study presents an unmanned airborne miniaturized pulsed CO_2 laser with wavelength automatic tuning. The mechanical Q-switching technology with fast chopper and the grating wavelength tuning technology driven by electric turntable were introduced. Without wavelength tuning modular, the mechanically Q-switched CO_2 laser had maximum peak power of 6.6 kW at 1 kHz with silt width of 0.8 mm, and the pulsed width was about 350 ns. With grating tuning, 37 lines were obtained in the range of 9.2 μm-10.71 μm. The maximum peak power was about 3.7 kW at 10.59 μm with a good beam quality ($Mx^2 \sim 1.65$, $My^2 \sim 1.74$). This laser had presented a good performance in the unmanned airborne environment.

Declaration of Competing Interest

The authors declare that they have no known competing financial interests or personal relationships that could have appeared to influence the work reported in this paper.

Acknowledgement

This study was supported by National Key R&D Program of China (2018YFE0203202), Youth Innovation Promotion Association CAS (2021216), Science and technology cooperation project between Jilin Province and Chinese Academy of Sciences (2021SYHZ0028), State Key Laboratory of Laser Interaction with Matter Project (SKLLIM1914, SKLLIM2115).

References

[1] Z. Cao, C. Wei, X. Cheng, Y. Zhao, X. Peng, Z. Jiang, J. Shao, Ground fused silica processed by combined chemical etching and CO_2 laser polishing with super-smooth surface and high damage resistance, Opt. Lett. 45 (21) (2020) 6014, https://doi.org/10.1364/OL.409857.

[2] S. Fan, N. Healy, CO_2 laser-based side-polishing of silica optical fibers, Opt. Lett. 45 (15) (2020) 4128–4131.

[3] T. He, C. Wei, Z. Jiang, et al., Numerical model and experimental demonstration of high precision ablation of pulse CO_2 laser, Chinese Optics Lett. 16 (4) (2018), 041401.

[4] R. Zhang, Q. Pan, J. Guo, F. Chen, D. Yu, J. Sun, K. Zhang, L. Zhang, Theoretical and experimental study of nanosecond pulse amplification in a CW CO_2 amplifier, Infrared Phys. Technol. 111 (2020) 103537, https://doi.org/10.1016/j.infrared.2020.103537.

[5] M.N. Polyanskiy, I.V. Pogorelsky, M. Babzien, M.A. Palmer, Demonstration of a 2 ps, 5 TW peak power, long-wave infrared laser based on chirped-pulse amplification with mixed-isotope CO_2 amplifiers, OSA Continuum 3 (3) (2020) 459, https://doi.org/10.1364/OSAC.381467.

[6] P. Ruan, Q. Pan, J. Xie, et al., Rapidly tunable pulsed CO_2 laser based on Acoustic-optic Modulator, Infrared Phys. Technol. 92 (2018) 299–303.

[7] M.K. Tehrani, M.M. Mohammad, E. Jaafari, A. Mobashery, Setting up a mobile Lidar (DIAL) system for detecting chemical warfare agents, Laser Phys. 25 (3) (2015) 035701, https://doi.org/10.1088/1054-660X/25/3/035701.

[8] C. Avishekh Pal, D. Clark, M. Sigman, et al., Differential absorption lidar CO_2 laser system for remote sensing of TATP related gases, Appl. Opt. 48 (4) (2009) 145–150.

[9] A.I. Karapuzikov, I.V. Ptashnik, I.V. Sherstov, et al., Modeling of helicopter-borne tunable TEA CO_2 DIAL system employment for detection of methane and ammonia leakages, Infrared Phys. Technol. 41 (2000) 87–96.

[10] L. Szinicz, History of chemical and biological warfare agents, Toxicology 214 (3) (2005) 167–181.

[11] F. Bandini, T.P. Sunding, J. Linde, O. Smith, I.K. Jensen, C.J. Köppl, M. Butts, P. Bauer-Gottwein, Unmanned Aerial System (UAS) observations of water surface elevation in a small stream: Comparison of radar altimetry, LIDAR and photogrammetry techniques, Remote Sens. Environ. 237 (2020) 111487, https://doi.org/10.1016/j.rse.2019.111487.

[12] J.H. Podoski, T.D. Smith, D.C. Finnegan, A.L. LeWinter, P.J. Gadomski, Unmanned aerial system lidar survey of two breakwaters in the hawaiian islands, Coast. Eng. (36) (2018) 23, https://doi.org/10.9753/icce:v36.structures.23.

[13] J. Xie, Q. Pan, R. Guo, L. Zhang, P. Ruan, D. Li, G. Yang, C. Zhang, J. Guo, Dynamical analysis of acousto- optically Q-switched CO_2 laser, Opt. Lasers Eng. 50 (2) (2012) 159–164.

[14] Y. Zhang, Z. Tian, Z. Sun, L. Wang, Q.i. Wang, Study of frequency stabilization for electro-optical Q-switched radio-frequency-excited waveguide CO_2 laser using build-up time method, Appl. Opt. 52 (16) (2013) 3732, https://doi.org/10.1364/AO.52.003732.

[15] A.N. Malov, A.M. Orishich, Ultimate Energy Characteristics of a Mechanically Q-Switched CO_2 Laser, Tech. Phys. Lett. 40 (2) (2014) 170–173.

[16] O. Svelto, Principles of Lasers, fifth ed., Springer, US, 2010.